
# NAVAL POSTGRADUATE SCHOOL

**MONTEREY, CALIFORNIA**

# THESIS

**OBJECTIVE IDENTIFICATION OF ENVIRONMENTAL PATTERNS RELATED TO TROPICAL CYCLONE TRACK FORECAST ERRORS**

by

Elizabeth Ravndal Sanabia

September 2006

Thesis Co-Advisors: Patrick A. Harr
Russell L. Elsberry

**Approved for public release; distribution is unlimited**

THIS PAGE INTENTIONALLY LEFT BLANK

| REPORT DOCUMENTATION PAGE | | | Form Approved OMB No. 0704-0188 |
|---|---|---|---|
| Public reporting burden for this collection of information is estimated to average 1 hour per response, including the time for reviewing instruction, searching existing data sources, gathering and maintaining the data needed, and completing and reviewing the collection of information. Send comments regarding this burden estimate or any other aspect of this collection of information, including suggestions for reducing this burden, to Washington headquarters Services, Directorate for Information Operations and Reports, 1215 Jefferson Davis Highway, Suite 1204, Arlington, VA 22202-4302, and to the Office of Management and Budget, Paperwork Reduction Project (0704-0188) Washington DC 20503. | | | |
| **1. AGENCY USE ONLY** ***(Leave blank)*** | **2. REPORT DATE** September 2006 | **3. REPORT TYPE AND DATES COVERED** Master's Thesis | |
| **4. TITLE AND SUBTITLE** Objective Identification of Environmental Patterns Related to Tropical Cyclone Track Forecast Errors | | | **5. FUNDING NUMBERS** |
| **6. AUTHOR(S)** Sanabia, Elizabeth R. | | | |
| **7. PERFORMING ORGANIZATION NAME(S) AND ADDRESS(ES)** Naval Postgraduate School Monterey, CA 93943-5000 | | | **8. PERFORMING ORGANIZATION REPORT NUMBER** |
| **9. SPONSORING /MONITORING AGENCY NAME(S) AND ADDRESS(ES)** N/A | | | **10. SPONSORING/MONITORING AGENCY REPORT NUMBER** |
| **11. SUPPLEMENTARY NOTES** The views expressed in this thesis are those of the author and do not reflect the official policy or position of the Department of Defense or the U.S. Government. | | | |
| **12a. DISTRIBUTION / AVAILABILITY STATEMENT** Approved for public release; distribution is unlimited. | | | **12b. DISTRIBUTION CODE** A |

**13. ABSTRACT**

The increase in skill of numerical model guidance and the use of consensus forecast techniques have led to significant improvements in the accuracy of tropical cyclone track forecasts at ranges beyond 72 h. Identification of instances when the forecast track from an individual numerical model may be in error could lead to additional improvement in the accuracy of tropical cyclone track forecasts. An objective methodology is tested to characterize the spread among the three primary global numerical model forecast tracks used as guidance by the Joint Typhoon Warning Center. Statistically-significant principal components derived from empirical orthogonal functions of mid-tropospheric height and vorticity forecast fields identify cases of large spread among model forecasts. Cases in which the three-model average forecast track resulted in a large error were characterized by a distribution of principal components such that one component was significantly different from the other two. Removal of the forecast track associated with the outlying principal component resulted in a reduced forecast error. Therefore, the objective methodology may be utilized to define a selective consensus by removing forecast tracks from consideration based on the projection of forecast fields onto empirical orthogonal functions and inspecting the distribution of the resulting principal components.

| **14. SUBJECT TERMS** Tropical Cyclones, Consensus Forecast Techniques, Principal Component Analysis, Objective Forecast Techniques | | | **15. NUMBER OF PAGES** 61 |
|---|---|---|---|
| | | | **16. PRICE CODE** |
| **17. SECURITY CLASSIFICATION OF REPORT** Unclassified | **18. SECURITY CLASSIFICATION OF THIS PAGE** Unclassified | **19. SECURITY CLASSIFICATION OF ABSTRACT** Unclassified | **20. LIMITATION OF ABSTRACT** UL |

NSN 7540-01-280-5500 Standard Form 298 (Rev. 2-89)
Prescribed by ANSI Std. 239-18

THIS PAGE INTENTIONALLY LEFT BLANK

**Approved for public release; distribution is unlimited**

# OBJECTIVE IDENTIFICATION OF ENVIRONMENTAL PATTERNS RELATED TO TROPICAL CYCLONE TRACK FORECAST ERRORS

Elizabeth R. Sanabia
Lieutenant Commander, United States Navy
B.S., United States Naval Academy, 1993

Submitted in partial fulfillment of the
requirements for the degree of

**MASTER OF SCIENCE IN METEOROLOGY AND PHYSICAL OCEANOGRAPHY**

from the

**NAVAL POSTGRADUATE SCHOOL**
**September 2006**

Author: Elizabeth R. Sanabia

Approved by: Patrick A. Harr
Thesis Co-Advisor

Russell L. Elsberry
Thesis Co-Advisor

Philip A. Durkee
Chairman, Department of Meteorology

THIS PAGE INTENTIONALLY LEFT BLANK

# ABSTRACT

The increase in skill of numerical model guidance and the use of consensus forecast techniques have led to significant improvements in the accuracy of tropical cyclone track forecasts at ranges beyond 72 h. Identification of instances when the forecast track from an individual numerical model may be in error could lead to additional improvement in the accuracy of tropical cyclone track forecasts. An objective methodology is tested to characterize the spread among the three primary global numerical model forecast tracks used as guidance by the Joint Typhoon Warning Center. Statistically-significant principal components derived from empirical orthogonal functions of mid-tropospheric height and vorticity forecast fields identify cases of large spread among model forecasts. Cases in which the three-model average forecast track resulted in a large error were characterized by a distribution of principal components such that one component was significantly different from the other two. Removal of the forecast track associated with the outlying principal component resulted in a reduced forecast error. Therefore, the objective methodology may be utilized to define a selective consensus by removing forecast tracks from consideration based on the projection of forecast fields onto empirical orthogonal functions and inspecting the distribution of the resulting principal components.

THIS PAGE INTENTIONALLY LEFT BLANK

# TABLE OF CONTENTS

THIS PAGE INTENTIONALLY LEFT BLANK

# LIST OF FIGURES

# LIST OF TABLES

THIS PAGE INTENTIONALLY LEFT BLANK

# ACKNOWLEDGMENTS

To my advisors, Professors Harr and Elsberry, I am especially grateful for your time, attention and guidance over the past several months. Professor Harr, thank you for your dedication, perspective and patience. Professor Elsberry, I am grateful for the standard you set and the fact that you will not settle for anything beneath it. I would also like to thank Grant Elliott, the Aussie, for your notable assistance with the data and database, as well as your ever-present sense of humor.

Finally to my family, I am very grateful for your unwavering support. Most especially to John and Amanda, you are the two most wonderful gifts I have ever been given. Thank you for your love, patience and willingness to camp out on my office floor. I am also grateful for the continuous reminders that you are to retain balance and perspective both at work and at home. I love you both with all my heart.

THIS PAGE INTENTIONALLY LEFT BLANK

# I. INTRODUCTION

## A. MOTIVATION

Accurately predicting the path of a tropical cyclone (TC) remains a formidable challenge to meteorologists today. Hurricanes are among the largest natural disasters and cause significant damage both on land and at sea. Over the western North Pacific Ocean, it is the responsibility of the Typhoon Duty Officer (TDO) at the Joint Typhoon Warning Center (JTWC) in Pearl Harbor, Hawaii, and his team to forecast the tracks and intensities of TCs for Department of Defense shore- and sea-based facilities. To construct an operational TC track forecast, the TDO relies on a variety of aids, which vary from statistical techniques to complex, global numerical forecast models. Often, the TDO is faced with the challenge of interpreting disparate guidance from these models.

The development and implementation of consensus track forecasting over the past decade have dramatically improved short-term tropical cyclone track forecasts (Goerss 2004). While near-term (12-72 h) track forecast accuracy has improved significantly over the past five years, accuracy of extended forecasts (96 and 120 h) has not improved substantially. In fact, the 120-h tropical cyclone track forecast errors have remained at approximately 300 n mi (Figure 1).

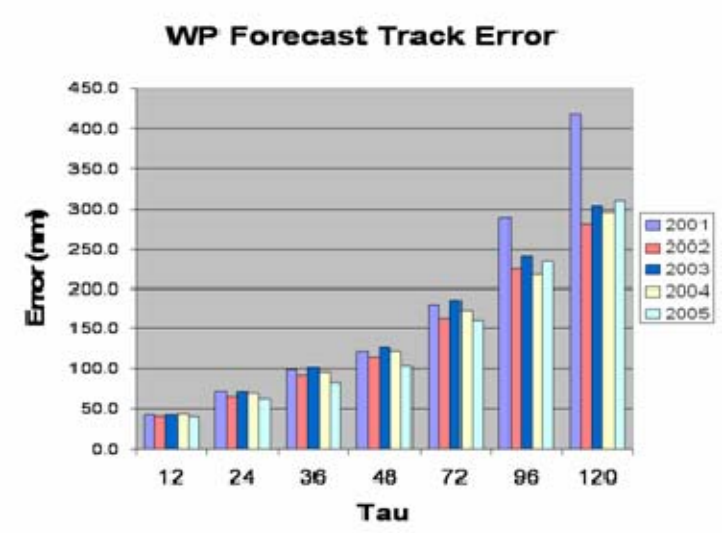


Figure 1. Joint Typhoon Warning Center 2001-2005 western North Pacific forecast official track errors (n mi) (personal communication, LCDR J. Dixon, 2006).

Improving 120-h track forecast accuracy will improve the ability of military disaster preparedness personnel to make sortie decisions for ships and aircraft. It will also enable civilian organizations to make evacuation recommendations for affected population centers, and thus mitigate risk and minimize damage.

## B. BACKGROUND

Several previous studies highlight the evolution and logical progression of TC track forecasting, which includes effective tools and techniques to minimize track error, and the requirement for an objective technique.

### 1. Consensus Forecasting – An Effective Error Reduction Technique

Goerss (2000) found that combining multiple models into a consensus forecast reduced TC track forecast error. Averaging the latitude and longitude (or geographic) forecast positions of separate operational models, which is labeled a non-selective consensus (N-CON), outperformed every individual model. The non-selective consensus is the baseline from which the JTWC initiates their TC track forecast process.

### 2. Selective Consensus – Reducing Error by Reducing Consensus Spread

Elsberry and Carr (2000) determined that narrowing the spread between forecast positions from different models improved TC track forecast accuracy at 72 h (the temporal limit of forecasts at that time). To narrow the spread, the forecaster analyzes the model fields and determines whether a model may not be predicting accurately the evolution of the large-scale environment, which would then be associated with an errant track. By identifying and eliminating an errant model track, the forecaster can form a "selective" consensus (S-CON) that will narrow the spread and reduce the forecast track error.

#### *a. Categorizing Error and Spread*

As indicated in the conceptual diagram in Figure 2, TC forecasts can be divided into four categories based on the spread among model tracks and the consensus forecast error. In small-spread, small-error (SSSE) cases, model guidance is consistent in that there is little variation among the model forecast tracks. The consensus lies within that group and the TC follows a path within the bounds of the model guidance. The result is small error and a good situation for forecasters.

In small-spread, large-error (SSLE) cases, the model track distribution exhibits small variability, but the actual TC track lies outside the boundaries of the model guidance, and thus a large consensus error results. This situation suggests that all models have made consistent errors, which would be difficult to recognize or interpret in a real-time forecast scenario.

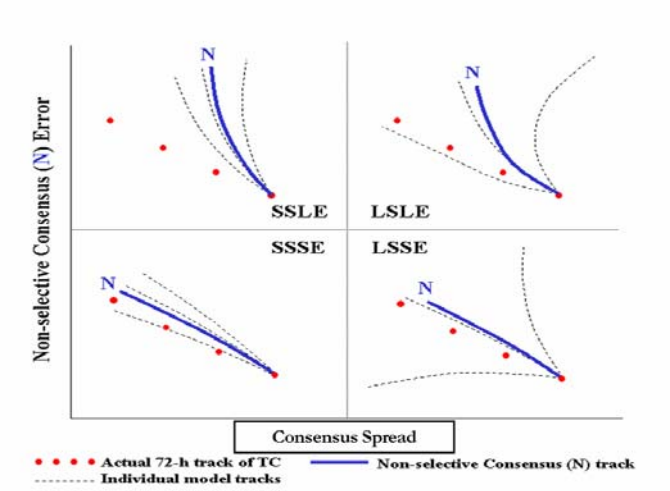


Figure 2. Conceptual diagram of spread vs. error (after Elsberry and Carr 2000)

Large-spread, small-error (LSSE) cases have less agreement among the model tracks, but the consensus splits the difference of the outliers and the actual TC track is close to the consensus track. In this case, there are usually compensating errors associated with the outlier tracks that cancel each other.

It is the large-spread, large-error (LSLE) cases that offer the greatest opportunity for improvement. In this case, the distance between forecast positions is great, and the actual TC track is near the predicted track of one of the outliers. It is this case that the forecaster may realize significant improvement if he/she is able to identify and eliminate the errant outlier track, as this will narrow the spread among model tracks and reduce the TC track forecast error of the consensus.

***b. Environmental Patterns – Identifying Error Mechanisms***

To determine the errant model track, recent efforts have focused on analyzing and identifying the causes behind large track forecast errors (Carr and Elsberry 2000a,b; Kehoe 2005; Payne 2006). In this way, it is expected that the forecaster can

identify these “error patterns” and eliminate the affected track. To support this endeavor, Carr and Elsberry (2000a,b) systematically described the environmental mechanisms that impact TC tracks. If these mechanisms are not represented properly in a model, there may be large errors in TC track forecasts.

An example of a relevant environmental mechanism is direct cyclone interaction (DCI, Figure 3). In this example of DCI, the TC approaches from the southeast (SE) and a second cyclone (of either midlatitude or tropical origin) approaches from the northwest (NW) and the two circulations begin to influence each other and then merge. As with all of these mechanisms, the occurrence of environmental patterns themselves may not result in an error. It is when the models do not predict them properly (denoted by “excessive” or “insufficient” in the systematic approach of Carr and Elsberry) that the difficulty arises.

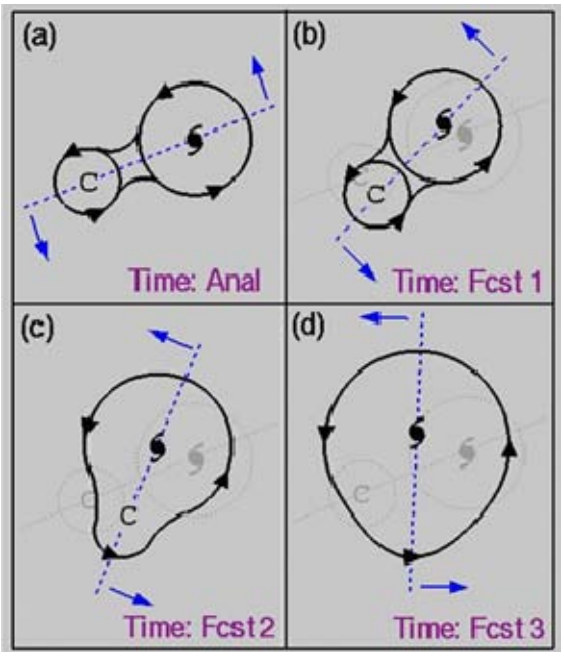


Figure 3. Schematic of the Direct Cyclone Interaction defined by Carr and Elsberry (2000a)

### *c. Challenges with Selective Consensus*

The inherent challenge for the forecaster is knowing when a model is developing a system excessively or insufficiently. In the previous example, excessive

DCI (E-DCI) would denote that the models merged the two systems (as in Figure 3) while in reality they did not. Two primary assumptions hinder the operational implementation of the selective consensus technique. The first is that the knowledge gained from hindsight from the previous year can be applied subjectively in real-time to subsequent storms. Second, it assumes the forecaster can discern between large-error and small-error cases when the spread among the model tracks is large (LSLE and LSSE) (Payne 2006). Because the JTWC forecasters could not apply the selective consensus approach to five dynamical models and significantly improve on a ten-model non-selective consensus at 72 h, selective consensus is no longer used as a forecasting technique by the JTWC (Sampson et al. 2006).

## C. PURPOSE

The purpose of this project is to reduce tropical cyclone track forecast errors at the longer forecast intervals by helping the forecaster identify which model may not be properly depicting the large-scale environment, and therefore should not be included in the consensus forecast.

This is not unlike other projects in its intent. Several previous studies have been undertaken to reduce forecast track error by identifying an errant model track using subjective interpretations based on past forecast performance (Carr and Elsberry 2000a,b; Kehoe 2005; Payne 2006). In these studies, all the large error cases were examined at the end of the season, and the environmental patterns were analyzed to determine why the errant model failed to handle the environmental pattern properly. A correlation between forecasts that resulted in large errors and the environmental patterns in which they occurred was established and made available for incorporation into the forecast process during follow-on seasons. While useful as an analytical and instructional tool, this method has proven difficult to employ operationally and is no longer utilized at the JTWC (Sampson et al., 2006).

Development of an alternate technique that utilizes a forward-looking, objective approach to correlate the environmental pattern to forecast track error may prove to be an effective and useful tool to reduce TC track forecast error. A benefit of this type of analysis is that it recognizes that large errors are not the singular result of prevalent

environmental patterns. Rather, it assesses all instances of a particular pattern and utilizes statistics to assess the outcome by using an objective technique to identify dominant environmental patterns and then determine if and how those patterns correlate to track forecast errors in the models. The problem is fundamentally based on spread about the consensus, as this and the model fields are the primary tools the forecaster has at his disposal.

This study is a counterpart to a previous thesis (Payne 2006) in which the large-error cases from the 2005 western North Pacific tropical cyclone season were examined subjectively to determine model error mechanisms. The difference between this and previous studies lies in the technique utilized to determine the errant model track. Previously, a subjectively-determined correlation has been defined between the actual error in the forecast track to the predicted environmental pattern. In this study, the purpose is to objectively determine the correlation between the forecast environmental pattern and the resulting model error.

# II. METHODS

## A. OVERVIEW

A priority in this study was to approach errant model track identification (and subsequent error reduction) from the viewpoint of the forecaster. Earlier retrospective studies focused on large error cases (the dashed line in Figure 4), determined how the model(s) had gone wrong, and assigned error mechanism(s) as appropriate. As mentioned previously, the challenge is that the forecaster has difficulty distinguishing between large and small error cases in real-time. The forecaster only knows the magnitude of the spread among the model tracks, which is defined to be either small spread (the left half of Figure 4) or large spread (the solid circle in Figure 4). It is the large error cases in which the forecaster needs the guidance to determine the errant track so that model guidance can be disregarded to form a selective consensus.

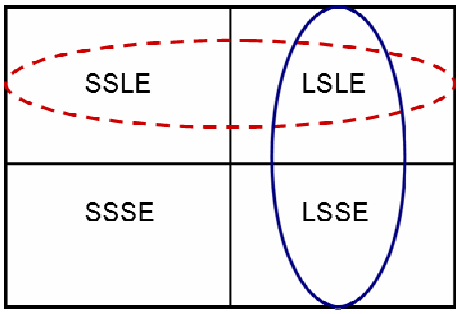


Figure 4. Conceptual model reflecting the change in approach from previous studies.

A second priority was to conduct a statistically-sound study. This priority impacted the division of the track error sample into terciles and the subsequent definitions of spread and error, which will be discussed in Chapter III.

The result of these priorities was a focus on the forward problem, which correlates statistical results of objectively-analyzed environmental patterns to their corresponding error magnitudes and model error mechanisms. To accomplish this, empirical orthogonal functions (EOFs) were utilized to characterize the environmental variability in the model over time. That is, the associated principal components (PCs) were utilized to describe

how many of the differences in the environment for a particular case could be attributed to a particular (environmental) pattern (i.e., EOF).

## B. DEFINITIONS

### 1. Consensus

Consensus position is defined in this study as the average latitude and average longitude of the three models.

### 2. Error

Several types of error are included in this study. Errors throughout the paper are given in nautical miles. Model error is the distance between an individual model forecast position and the best-track position. Mean model error is calculated by averaging the three individual model errors. The consensus error is determined by calculating the distance between the consensus forecast location and the best-track position.

Previous subjective studies (Carr and Elsberry 2000a,b; Kehoe 2005; Payne 2006), had established large error benchmarks as: 300 n mi for 72 h, 400 n mi for 96 h, and 500 n mi for 120 h. Since this was an objective study, statistical methods were appropriate. The mean model error for each case was calculated and tercile boundaries were determined to subdivide the cases into small, medium, and large error categories.

### 3. Spread

As with error, there are several types of spread considered in this study, and they are also given in nautical miles. The mean model-to-best-track spread is defined by the standard deviation of the distance between each model forecast position and the best-track position. The mean model-to-consensus spread is the standard deviation in the distance between each model forecast position and the consensus. The mean model-to-consensus spread is analyzed in this study to define terciles of the spread (small, medium, large).

## C. DATA

The focus region for this study was the western North Pacific for the 2005 season, where 25 TCs occurred. The JTWC Best Track database was used as the ground truth for tropical cyclone positions and intensities.

Although at least ten techniques or models provide 72-h forecast tracks in the western North Pacific, only four models (the Global Forecast System (GFS), Navy Operational Global Atmospheric Prediction System (NOGAPS), United Kingdom Meteorological Office (UKMO), and Geophysical Fluid Dynamics Laboratory–Navy version (GFDN)) provide 96-h and 120-h forecast fields. Due to data availability constraints, three global models (GFS, NOGAPS, and UKMO) were utilized in this study. Because of constraints in the approach, a homogenous set was required such that forecasts from all three models had to be available for a case to be included in this study. Furthermore, all forecasts had to have a verifying 120-h position.

Because of operational global model time delays, tracks from the 0000 UTC and 1200 UTC model forecasts are interpolated to 0600 UTC and 1800 UTC positions for use with the 0600 UTC and 1800 UTC forecast products. However, the original model fields at the 0000 UTC and 1200 UTC initial times are used in this study.

The model fields were processed on a one-degree latitude-longitude grid. Seven variables were considered: 500 hPa height, 500 hPa vorticity, 1000-500 hPa thickness, sea-level pressure, 700 hPa height, 700 hPa vorticity, and 200 hPa vorticity. For each variable at each time step, the original fields for each model were re-aligned to a 51x51 degree grid with the storm placed off-center, such that it was 31 degrees longitude from the western boundary and 21 degrees latitude from the southern boundary. At each grid point, a three-model average was defined and a difference field was constructed for each model by subtracting the three-model average from the individual model fields (Figure 5).

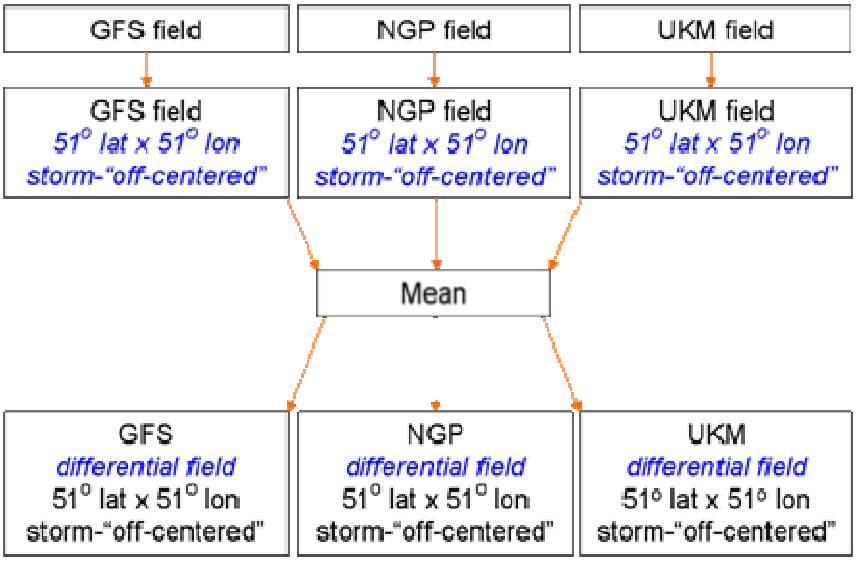


Figure 5. Schematic of the data processing stages for each model.

The example given in Figure 6 depicts an original NOGAPS 500 hPa vorticity analysis trimmed to the 51x51 grid size (Figure 6a). The center of positive vorticity is evident at the (31,21) position. After subtracting the three-model average, the differential vorticity chart is defined (Figure 6b).

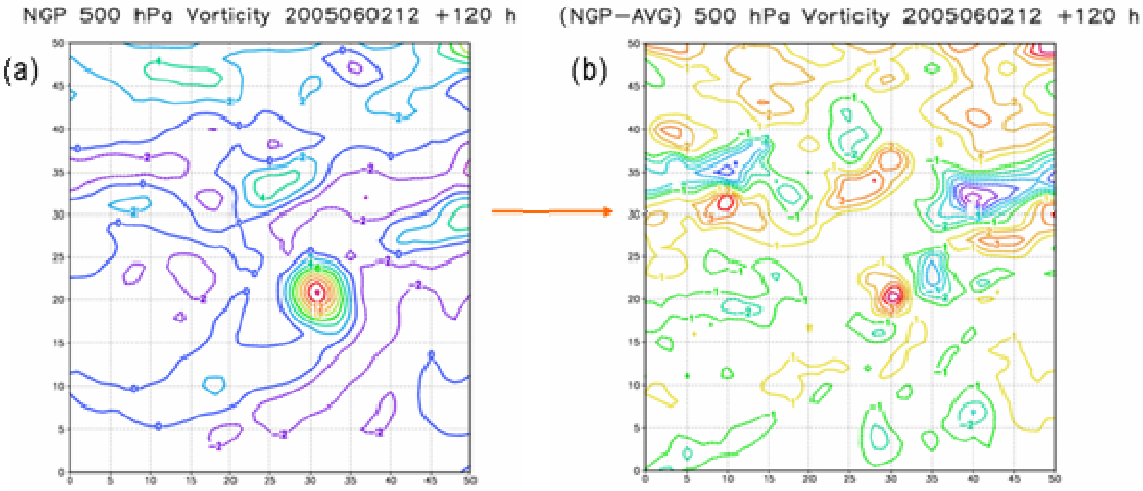


Figure 6. Depiction of an (a) original realigned 120-h NOGAPS 500 hPa relative vorticity ($10^{-5}$ $s^{-1}$) and (b) differential vorticity field ($10^{-5}$ $s^{-1}$).

## D. ANALYSIS TOOLS AND TECHNIQUE

### 1. Empirical Orthogonal Functions

The data preparation procedure in Figure 5 is followed for each variable in each model at each time step. The anomaly fields are then input to the EOF procedure. The multivariate EOF technique (Richman 1986) is used to define the underlying spatial structures that best explain the variability in each model represented by each variable at each forecast time. The EOF analysis was performed on a covariance matrix constructed from the set of 51x51 grids for each model, field, and forecast interval. Because of the requirement for a homogeneous set of cases, the number of cases varied with forecast interval and ranged from 96 at 72 h to 35 at 120 h. For each model, field, and time, the most common spatial pattern of variability is defined by the first EOF mode, which explains the maximum amount of variance about the mean. The second EOF pattern represents the second-most common spatial structure that maximizes the variance about the mean once the variability accounted for by the first EOF has been removed. The EOFs are ordered such that the greatest variability is characterized by the pattern given in EOF1, and this variability decreases with each subsequent EOF.

A set of EOF patterns for 120-h forecasts of 500 hPa relative vorticity is given in Figure 7. Although the number of EOFs is set by the number of grid points (i.e., 51x51), only the first three are considered in this study. The percent on the top right of each chart indicates the amount of variance in the variable that is explained by that particular pattern. Since vorticity is a highly variable field, the variance is widely spread among the EOFs. However, the heights contain less variability and typical values of explained variance for the leading modes were near 40%.

Because the three-model average has been subtracted, each EOF pattern delineates a partial contribution to the forecast motion of the TC that deviates from the consensus position. That is, the pattern in each EOF reflects how that model varies from the 3-model average for that variable at that time. The steering flow that results from any such pattern is therefore different from the flow represented by the three-model average.

The subsequent effect on the model-predicted TC motion will be a deviation from the consensus (average) position in the direction prescribed by the summation of all the EOFs.

## 2. Principal Components

By projecting the EOFs onto the original data, a principal component (PC) is defined that denotes the weight of each EOF in each case (Figure 8). Because the mean of the PCs is zero and the standard deviation is one, statistically-significant PC amplitude is defined to be greater than 1.0 or less than -1.0.

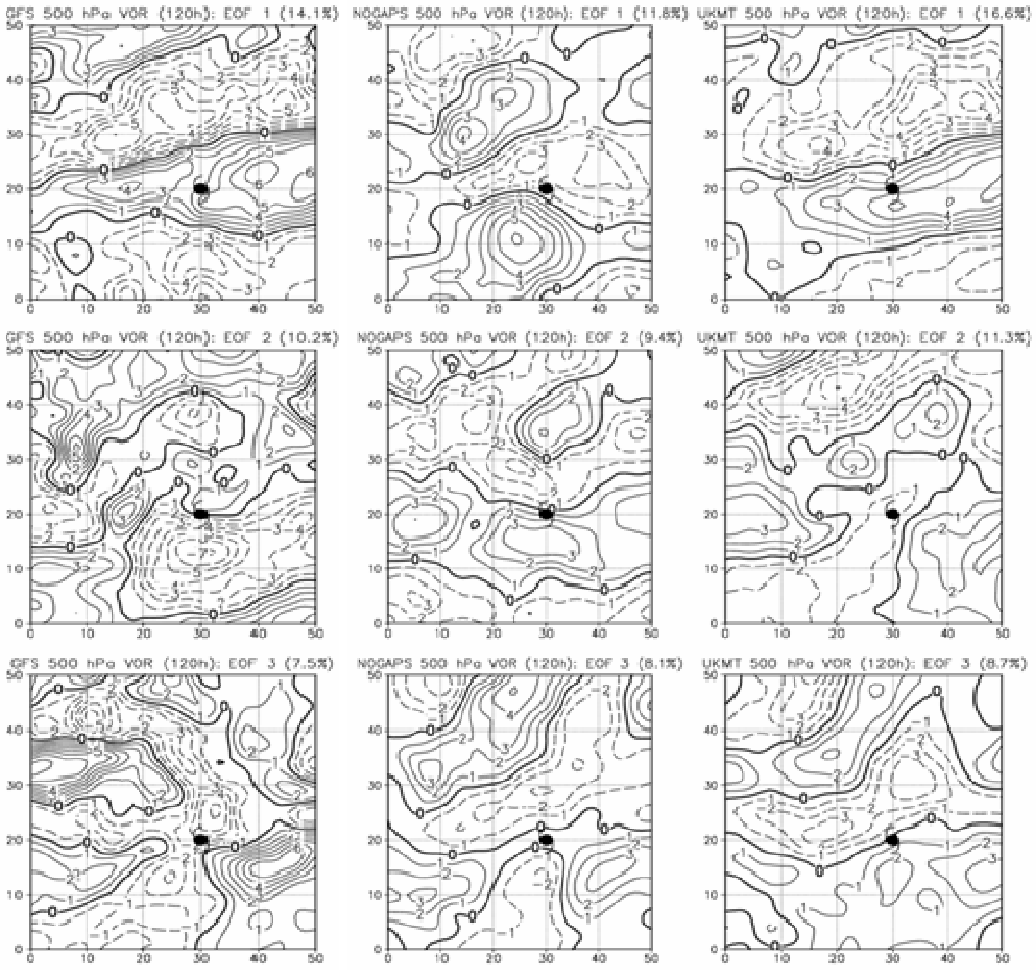


Figure 7. Empirical Orthogonal Functions (EOFs) for 500 hPa vorticity ($10^{-5}$ $s^{-1}$) at 120 h. The GFS, NOGAPS, and UKMO models are in columns 1-3, respectively, and EOFs 1-3 are ordered in rows. The percent variance explained by each EOF is listed at the top right corner of each chart. The thick black line is the zero line, the solid lines are positive and the dashed lines are negative.

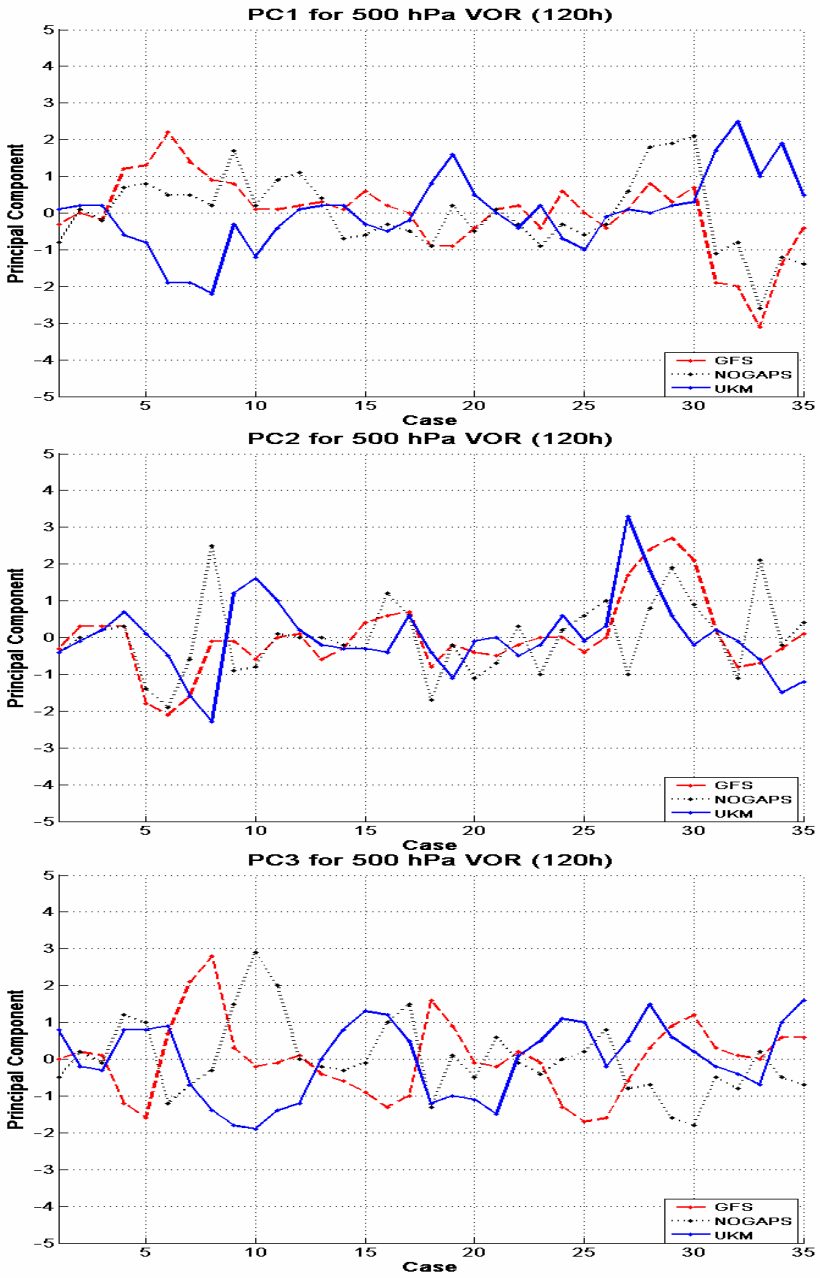


Figure 8. Principal Components (PCs) 1-3 for 500 hPa vorticity at 120 h. The 35 cases are listed chronologically on the x-axis and the PC magnitude is on the y-axis. GFS is denoted in red, dashed lines, NOGAPS in black, dotted lines and UKMO in blue, solid lines.

As an example, the peak in the amplitude of the UKMO 500 hPa vorticity PC1 at 120 h for case 32 (Figure 8) indicates a large amount of weight on UKMO EOF1 (Figure 7, upper right). Based on a large positive weight on the EOF1 UKMO 500 hPa vorticity chart, the storm is in a region of positive vorticity, and the corresponding counterclockwise (CCW) circulation that is coupled with the clockwise (CW) circulation of the region of negative vorticity to the north implies a steering flow toward the west. Consequently, the UKMO vorticity deviates from the mean 500 hPa vorticity of the three models in this case such that its forecast large-scale pattern induces a more westward component to the TC motion.

A reversal in the sign of the PC reverses the sense of the EOF pattern, i.e., positive regions become negative and gradients are reversed. For example, the UKMO EOF1 PCs in Figure 8a are negative in cases 7-9, so the positive and negative areas on the EOF1 are reversed in sign. The storm is now in an area of negative vorticity with positive vorticity to the north and the effect on the storm is steering toward the east.

## 3. Analysis Technique

To correlate environmental patterns to TC track errors, the initial step is to examine statistically-significant PCs for each model. In this study, these cases were then compared to the corresponding TC track errors to determine case dependency to the various scales of error and spread, and then to isolate cases for further examination. For each case chosen, the amplitude of the PC was correlated to the steering flow indicated by the EOF spatial pattern. Although the EOF represented the influence of one parameter at one level of the atmosphere, the direction of this "expected" error was compared to the direction of the actual error (defined as the direction from the best-track position to the model forecast position). It is understood that the steering flow prescribed by the EOF pattern will describe movement away from the consensus position, and that it is instead being correlated to actual bearing error, which is in comparison to the best track. As an initial study, this aspect of the procedure was acknowledged as an accepted, although potentially limiting, practice. With the magnitude and direction of the error understood, model fields were examined to determine the possible error mechanism. References to Payne (2006) were made to (independently) confirm error mechanism assignments.

Once the statistically-significant peaks in the PCs for individual cases were initially correlated to error mechanisms, two additional steps were taken to determine the prevalence and depth of the signal and to determine the exclusivity of the correspondence. Subject cases were investigated for statistically-significant PCs through the first three PCs for four variables (500 hPa heights, 500 hPa vorticity, 700 hPa heights and 700 hPa vorticity) at the 120-h time step. These four variables were selected because of their impact on TC steering and clarity of their EOF patterns. The initial procedure for determining error magnitude and direction as described in the previous paragraph was followed for each of these cases. Then, exclusivity of the PC signal-to-error-mechanism correlation was determined by examining other statistically-significant PCs of the same sign and determining if similar errors occurred in those cases, and whether or not those errors were caused by the same error mechanisms.

THIS PAGE INTENTIONALLY LEFT BLANK

# III. RESULTS

## A. ERROR VERSUS SPREAD

Statistical analysis of the 35 cases in the 120-h data set provided information from which to begin correlating environmental patterns to model errors. Eight of the 25 TCs that occurred during the 2005 western North Pacific TC season were represented in the data for this study with between two and eight forecasts per storm. Division of the mean model error into terciles provided the following error thresholds: small error (SE) < 210.7 n mi, SE < medium error (ME) < 280.9 n mi, large error (LE) > 280.9 n mi. Division of the model-to-consensus spread into terciles yielded the following spread thresholds: small spread (SS) < 41.6 n mi; SS < medium spread (MS) < 88.9 n mi; large spread (LS) > 88.9 n mi (Table 1). One consequence of the differences in definitions between this study and its subjective predecessors was that only 11 of the 105 individual forecasts composing this 120-h data set met the "large error" definition of those previous studies (> 500 n mi). As a result, only those 11 were assigned error mechanisms in the Payne (2006) study.

Table 1. Division of 120-h cases within mean-model-error and consensus spread terciles.

| 120-h Cases | Small Spread (SS) (SS < 41.6 n mi) | Medium Spread (MS) (41.6 n mi < MS, & MS < 88.9 n mi) | Large Spread (LS) (LS > 88.9 n mi) | Grand Total |
|---|---|---|---|---|
| **Large Error (LE)** (LE > 280.9 n mi) | 2 | 3 | 7 | 12 |
| **Medium Error (ME)** (210.7 n mi < ME < 280.9 n mi) | 5 | 3 | 3 | 11 |
| **Small Error (SE)** (SE < 210.7 n mi) | 5 | 5 | 2 | 12 |
| **Grand Total** | 12 | 11 | 12 | 35 |

The case count in Table 1 reveals that large-spread (LS) cases typically resulted in large errors. Seven LE cases, three ME cases, and two SE cases composed the LS category. The error-and-spread divisions (Table 1) also indicate that large errors

occurred predominantly in large spread cases. There were seven LE cases in the LS category, three LE cases in the MS category, and two LE cases in the SS category.

Examination of the mean-model error for each spread category indicates that this error increased significantly from the small- and medium-spread errors to the large-spread cases (Table 2). Since the average model error of large-spread cases exceeded that of medium- and small-spread cases by more than 100 n mi, focusing on these cases offers the greatest opportunity for reduction in track forecast error, as previously described. Associating these errors with individual cases (Table 3) provides the background required for effective analysis of the EOFs and PCs.

Table 2. Average model error for each consensus-spread tercile.

| Model-to-Consensus Spread Category | Average Model Error (n mi) |
|---|---|
| Large Spread | 364.2 |
| Medium Spread | 234.5 |
| Small Spread | 239.9 |
| Average 120-h error | 280.8 |

Table 3. Case numbers within each consensus-spread and mean-model-error tercile.

| | | |
|---|---|---|
| **SSLE**<br>16,26 | **MSLE**<br>7,17,28 | **LSLE**<br>4,5,6,8,29,30,33 |
| **SSME**<br>12,13,19,24,25 | **MSME**<br>27,31,35 | **LSME**<br>20,32,34 |
| **SSSE**<br>9,14,15,18,23 | **MSSE**<br>1,10,11,21,22 | **LSSE**<br>2,3 |

## B. EOF AND PC ANALYSIS

Intuitively, the variation in the amplitudes of the PCs for the three models should correspond directly to the spread among the individual model tracks. If the three model fields are very similar, (i.e., small PC values) none of the three models will have a strong "differential" pattern and therefore those patterns will not correlate strongly to the EOFs. When the fields are vastly different, the signals of the differential fields will be very strong, and the correspondence of those fields to EOFs should be high and result in high-amplitude PCs.

It was anticipated that each model would exhibit somewhat consistent spatial patterns of variability for each EOF. However, this occurred only rarely in the 72-h, 96-h, and 120-h EOF charts. Patterns of variability were much more likely to be similar for two of the three models, but for different models in EOFs 1-3. A potential cause for the lack of similarity among EOF patterns is the small sample size used to construct the EOFs. Increasing the number of cases by including additional years will lead to more stability in the EOF pattern. This made the analysis procedure slightly more involved, as it was initially believed that error assessments could be made based on varying degrees of correspondence (differing PC magnitudes) for each model to a similar EOF pattern. As this was not the case, the procedure described in Chapter II.D.3 was developed and implemented.

**1. 500 hPa Height**

The 500 hPa height EOFs (Figure 9) tended to reveal deviations from the three-model average synoptic patterns more clearly than any of the other variables. The dominant EOF1 environmental patterns are similar for GFS and NOGAPS, with regions of higher heights to the south and to the west, and lower heights to the north and to the east when the PC1 is positive. The primary difference between GFS and NOGAPS in EOF1 is the position of the TC relative to the trough. In EOF1 for the GFS, the TC is along the trough axis. In NOGAPS, the trough axis is not as steep and the TC is west of the axis. The EOF1 pattern for the UKMO model has a different orientation and weaker gradients compared to the other models.

Examination of EOF2 (Figure 9) reveals the environmental patterns that often impact TC steering. The EOF patterns in the GFS and NOGAPS have the TC south of a gap in heights, which corresponds to a break in the subtropical ridge when PC2 is positive. The EOF2 pattern for the UKMO is more comparable to the NOGAPS EOF1 pattern, with the TC along the trough axis. For EOF3, the patterns in Figure 9 for the GFS and the UKMO models are most similar, with higher heights to the west and lower heights to the east when PC3 is positive. Although the pattern in NOGAPS is somewhat similar, the region of higher heights to the west extends closer to the TC position in the NOGAPS PC3.

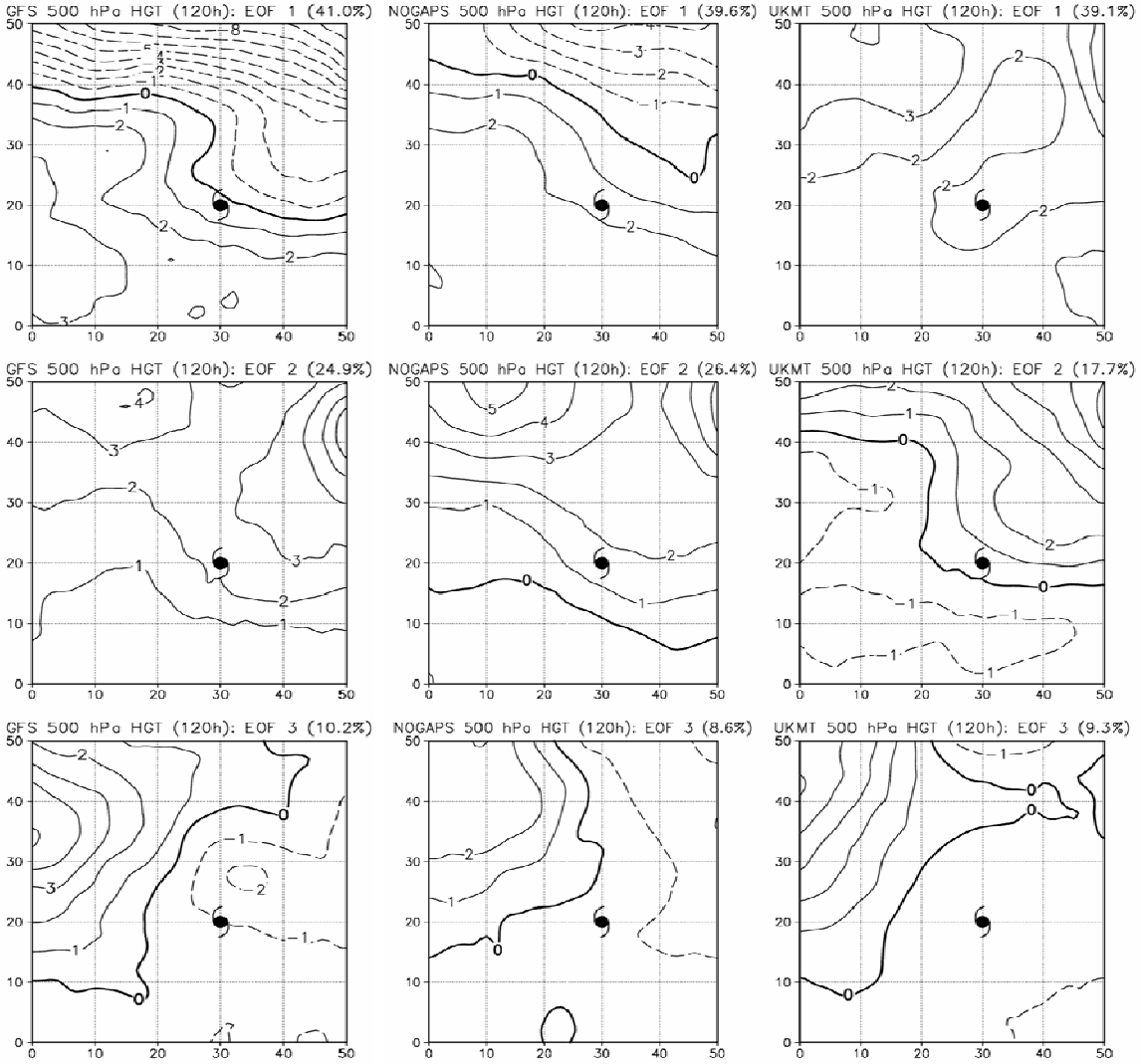


Figure 9. Empirical Orthogonal Functions (EOFs) for 500 hPa height at 120 h. The GFS, NOGAPS, and UKMO models are in columns 1-3, respectively, and EOFs 1-3 are ordered in rows. The percent variance explained by each EOF is listed at the top right corner of each chart. The thick black line is the zero line, the solid lines are positive and the dashed lines are negative. Contour interval is 1 m.

The tendency for two of the three models to exhibit similar EOF patterns is also evident in the PC coefficients. Often, when large differences exist among coefficients for individual cases, the difference is due to one extreme-valued PC with the other two coefficients being similar in sign and magnitude. Examples of these characteristics include cases 31-33 for PC1 (Figure 10, top) and 5-7 for PC2 (Figure 10, middle).

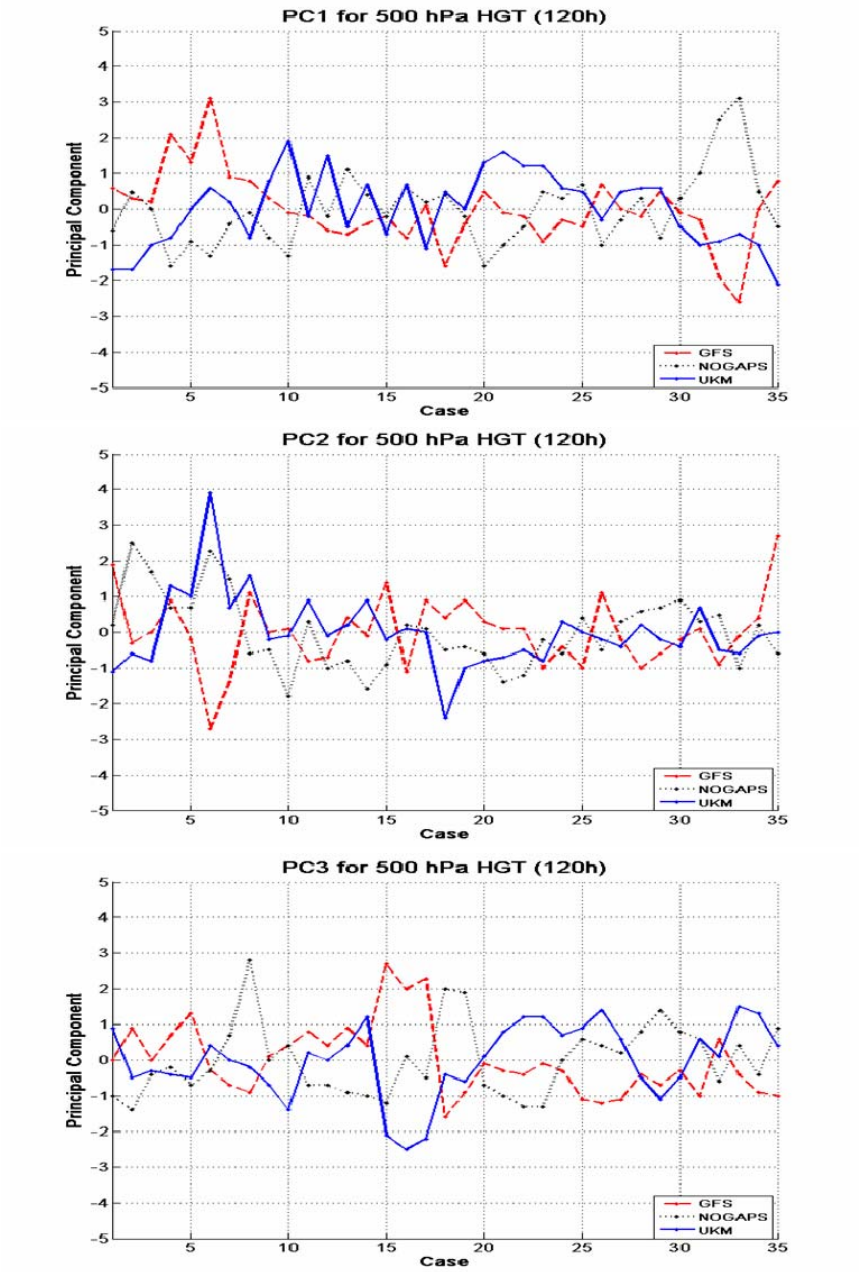


Figure 10. Principal Components (PCs) 1-3 for 500 hPa height at 120 h. The 35 cases are listed chronologically on the x-axis and the PC magnitude is on the y-axis. GFS is denoted in red, dashed lines, NOGAPS in black, dotted lines and UKMO in blue, solid lines.

The distribution of PCs for each case also provides an indication of the spread among models. A comparison of the LS cases listed in Table 3 with the PC1 values in Figure 10 indicates that except for cases 29 and 30, at least one PC is separate from the

others. When more statistically-significant PCs exist in an individual case, there tends to be greater spread between individual models. For example, eight of the 35 cases have two models with statistically-significant PC1s. Of those eight, five are large-spread cases and three are medium-spread cases (Figure 10). While this does not confirm that small-error cases will have small amplitude PCs, it does confirm that medium- and large-spread cases are more apt to have multiple statistically-significant PCs.

Of particular interest was that in the small-spread cases, the variability in the 500 hPa heights appeared to be more evident in higher numbered EOFs, and the quantity of statistically-significant PCs increased with each EOF. Cases 14-16, which are all SS cases (14 and 15 are SE cases, 16 is a LE case), highlight this feature (Figure 10). In PC1, there are no statistically-significant amplitudes for 500 hPa heights in these three small-spread cases. In PC2, the amplitude of the PCs in cases 14-16 increases and three of the nine amplitudes are statistically significant. Furthermore, eight of the nine peaks in PC3 are statistically significant. The amplitude of the PCs in these small-spread cases increased as the amount of explained variance decreased.

**2. 500 hPa Vorticity**

The EOF1 patterns of 500 hPa vorticity (Figure 7) define a typical monsoon trough/subtropical ridge environment of the western North Pacific. In each pattern, a zonally–oriented vorticity center is present that varies by longitude. The primary differences among the three patterns lie in where the TC is located with respect to the circulation. The EOF1 patterns for NOGAPS and GFS have the TC near the zero line of opposite-signed vorticity centers. The GFS pattern has the TC in the middle of a positive vorticity center if PC1 is positive. Therefore, this pattern identifies how the models might differ in their representation of the primary large-scale vorticity centers over the western North Pacific.

Less agreement exists among EOF2 patterns (Figure 7), although both the GFS and NOGAPS patterns place the TC north of positive vorticity centers when PC2 is positive. Additionally, NOGAPS and UKMO both have vorticity centers extending northeast-to-southwest north of the TC. This agreement extends into the EOF3 patterns,

in which NOGAPS and UKMO both have a northeast-southwest oriented vorticity center that seems representative of a midlatitude trough extending toward the TC when PC3 is positive.

Similar to the PCs of 500 hPa height in Figure 10, small-spread cases listed in Table 3 tend to show little separation among the PC1 values for 500 hPa vorticity (Figure 8) with no statistically-significant PCs in the small-spread cases 14-16, but increasing amplitudes in PC2 (to one of nine) and PC3 (to four of nine). Medium-spread and large-spread cases again reflected the tendency to have multiple statistically-significant PC amplitudes. Six of the 35 cases had multiple statistically-significant PC1s, two in MS cases and four in LS cases. While the association with large spread is also evident in the case-to-case variability among PCs, the coefficients for 500 hPa vorticity (Figure 8) reflect that often two of the three models agree on their representation of the large-scale pattern of vorticity over the western North Pacific.

### 3. 700 hPa Height

The synoptic patterns in the leading EOFs for 700 hPa heights (Figure 11) are not as well defined as those noted for 500 hPa heights (Figure 9). Although between 35-40% of the variability in each model is contained in its respective EOF1, each model has a different pattern. The second EOFs of 700 hPa heights are well-defined patterns for each model. A strong similarity between the pattern for the GFS and NOGAPS models is that the TC is between an area of higher heights to the northeast and lower heights to the southwest when PC2 is positive. The pattern for the UKMO model is quite different in that it defines a more zonal height distribution. The agreement between the NOGAPS and UKMO patterns is less well-defined, but still present in the patterns for EOF3. When PC3 is positive, these two models both have high height centers to the north-northwest (NNW) of the TC position, whereas the GFS also has a region of higher heights, and its relative position is west-northwest (WNW) of the TC.

The distribution of PCs for 700 hPa heights (Figure 12) is not very clear in that there is no indication of the LS cases in Table 3. Except for a very few number of cases (14-16, which are small-spread cases, in PC1), the amplitudes of most PCs are consistent, or are evenly distributed between -1 and 1 such that there is no indication that any one

model is significantly different from the other two. This suggests that 700 hPa heights may not be a field that varies significantly among the three models.

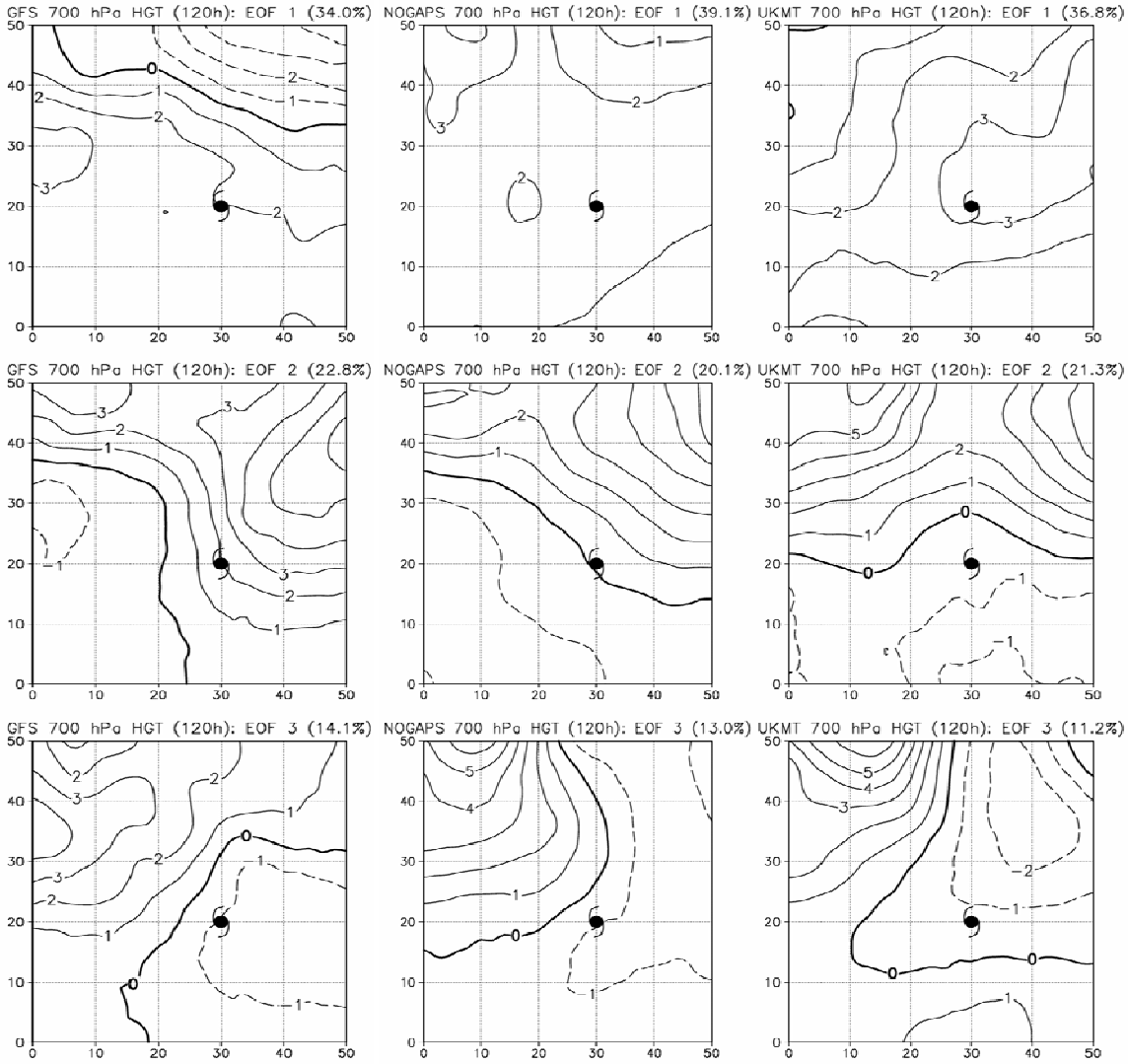


Figure 11. Empirical Orthogonal Functions (EOFs) for 700 hPa height at 120 h. The GFS, NOGAPS, and UKMO models are in columns 1-3, respectively, and EOFs 1-3 are ordered in rows. The percent variance explained by each EOF is listed at the top right corner of each chart. The thick black line is the zero line, the solid lines are positive and the dashed lines are negative. Contour interval is 1 m.

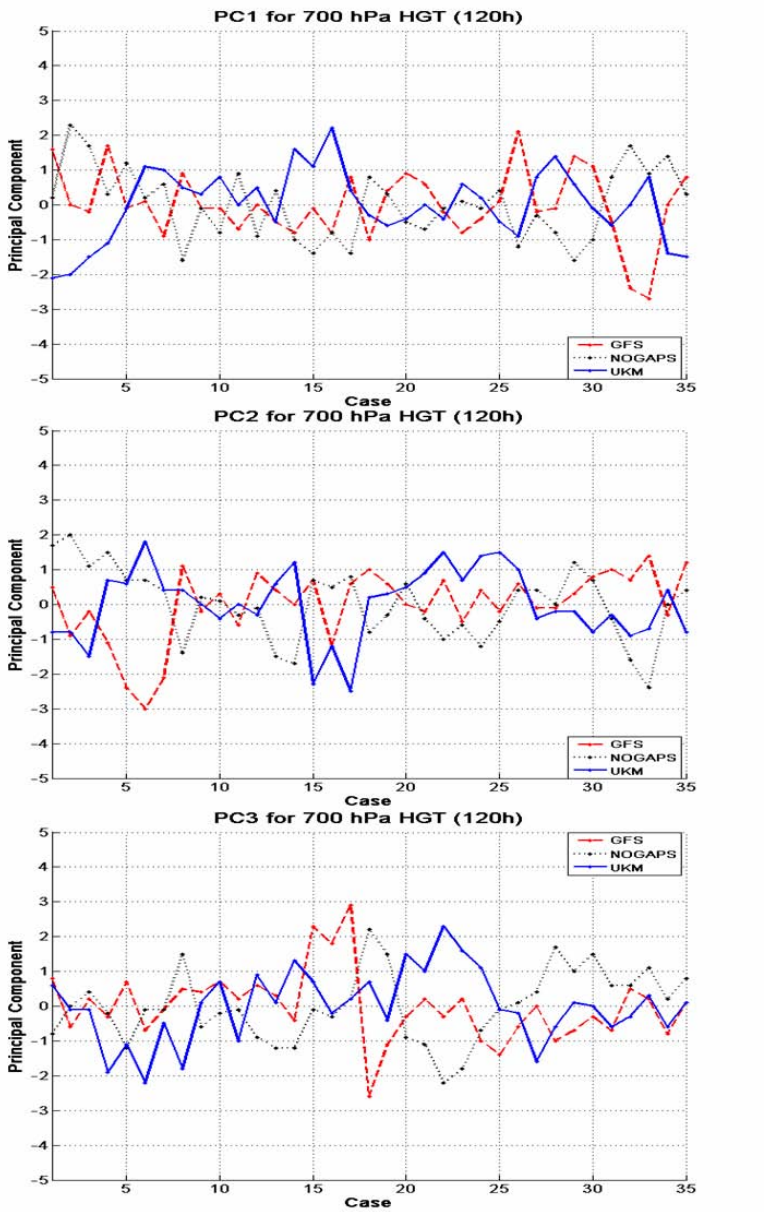


Figure 12. Principal Components (PCs) 1-3 for 700 hPa height at 120 h. The 35 cases are listed chronologically on the x-axis and the PC magnitude is on the y-axis. GFS is denoted in red, dashed lines, NOGAPS in black, dotted lines and UKMO in blue, solid lines.

### 4. 700 hPa Vorticity

As with the 500 hPa vorticity (Figure 7), the variability accounted by each EOF pattern in 700 hPa vorticity (Figure 13) is more evenly distributed among the EOFs, with about 10% explained in each model's EOF1. In each of the EOF1 patterns, the TC lies

between a positive vorticity area to the south and a negative area to the north when PC1 is positive. This is the best agreement among all three patterns of the variables thus far.

For EOF2 (Figure 13), the patterns associated with the NOGAPS and UKMO models both define two meridionally-oriented circulation centers to the north of the TC. However, the EOF pattern of the GFS is a more zonally-oriented circulation.

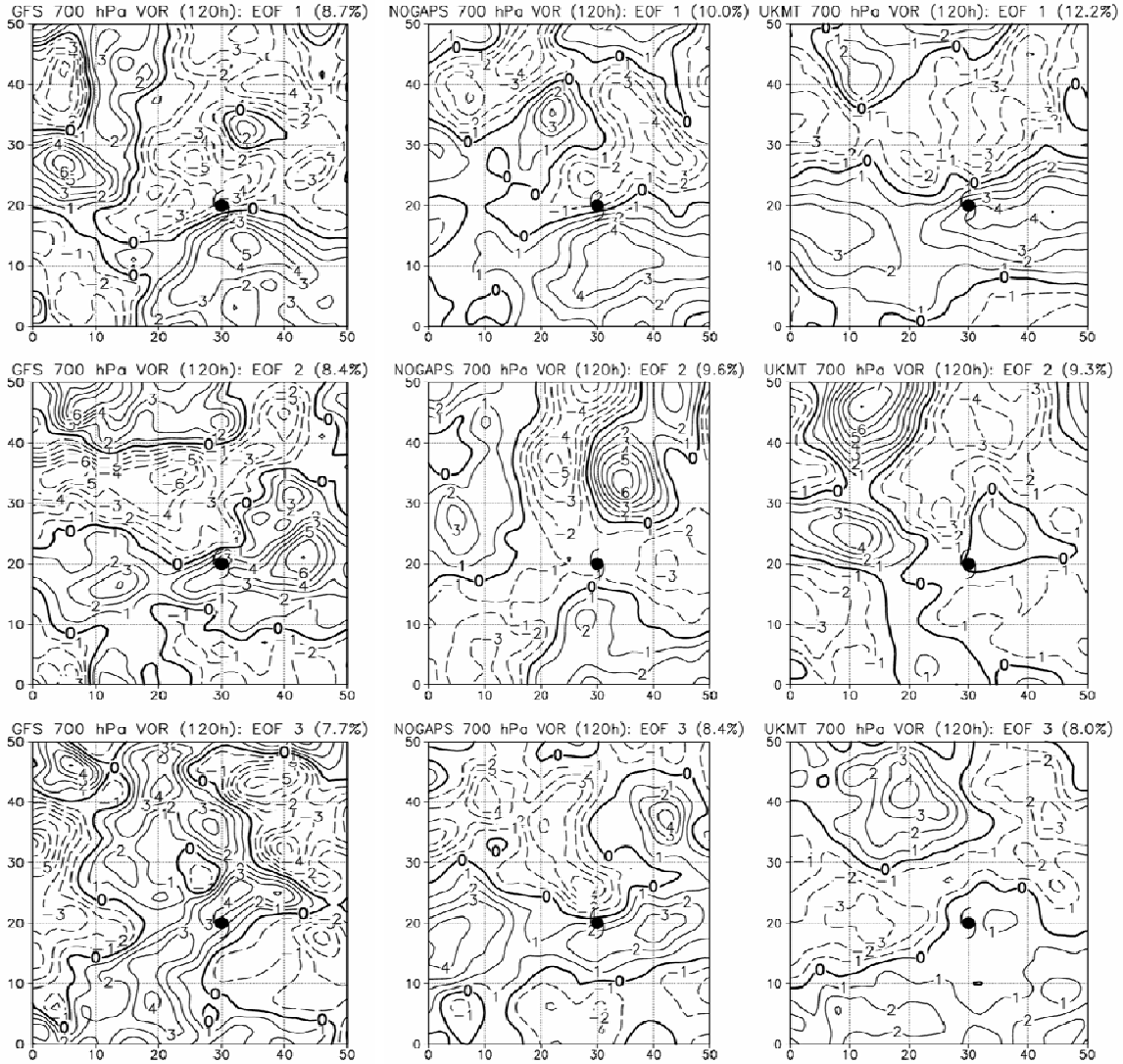


Figure 13. Empirical Orthogonal Functions (EOFs) for 700 hPa vorticity ($10^{-5}$ $s^{-1}$) at 120 h. The GFS, NOGAPS, and UKMO models are in columns 1-3, respectively, and EOFs 1-3 are ordered in rows. The percent variance explained by each EOF is listed at the top right corner of each chart. The thick black line is the zero line, the solid lines are positive and the dashed lines are negative.

For EOF3 (Figure 13), the pattern for the UKMO and NOGAPS models are similar in that the TC is near the boundary of a positive vorticity center to the south and a negative vorticity center to the north when PC3 is positive. The pattern associated with the GFS model contains many small-scale features with a quadrapole of vorticity centers clustered to the north of the TC.

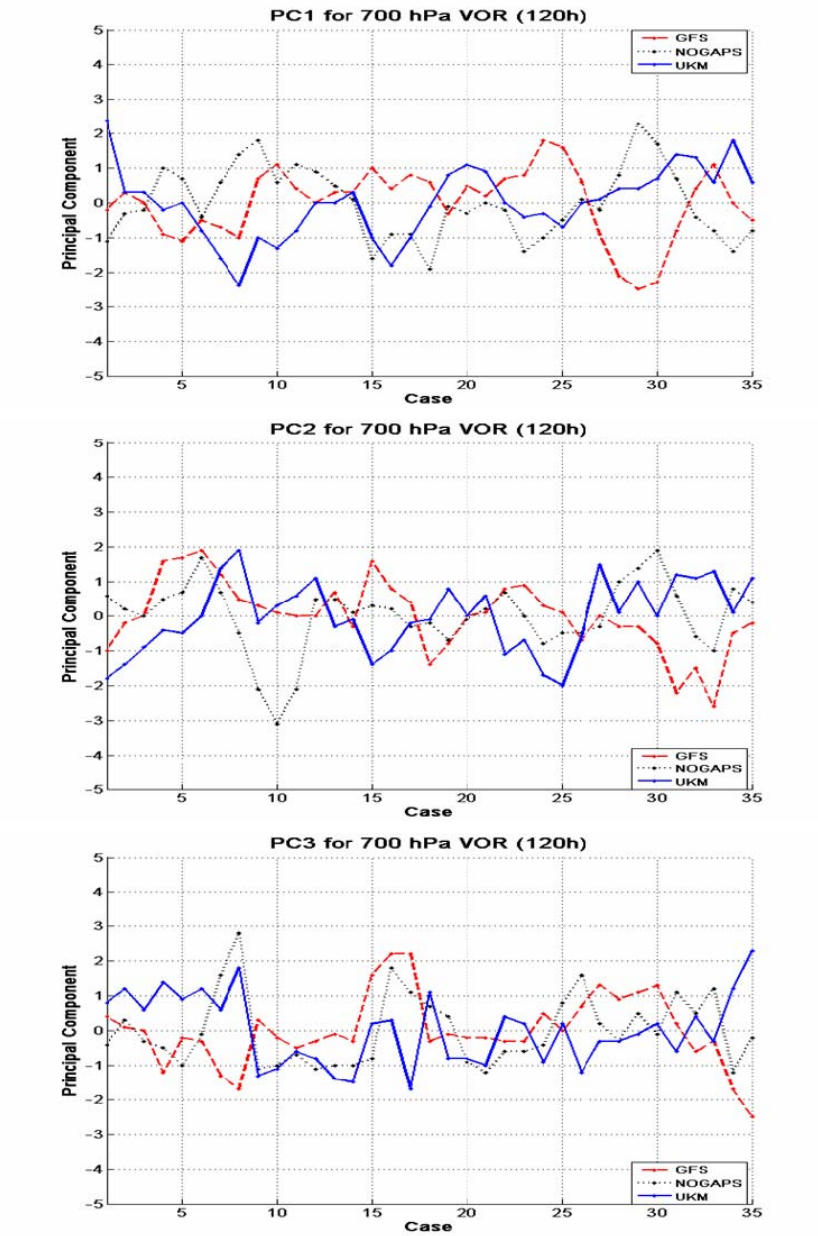


Figure 14. Principal Components (PCs) 1-3 for 700 hPa vorticity at 120 h. The 35 cases are listed chronologically on the x-axis and the PC magnitude is on the y-axis GFS is denoted in red, dashed lines, NOGAPS in black, dotted lines and UKMO in blue, solid lines.

The associations that PCs have had with the model spread cases discussed above do not hold well for 700 hPa vorticity (Figure 14). Medium- and large-spread cases do not correlate well with the multiple-statistically-significant PC category. For the nine cases with multiple-significant PC amplitudes, three are SS cases, four are LS cases, and two are MS cases.

### 5. Summary

The inference from this distribution of EOFs and PCs is that large-spread cases should have high correspondence to EOF patterns that deviate from the mean, and therefore the differenced fields should have strong correlation to various EOF patterns. The question then is how does one determine whether a high-amplitude PC (with a large correlation to an EOF pattern) indicates that the model is predisposed to a large error? For 500 hPa height EOFs, a case count reveals that, of the 29 times individual models had statistically-significant PC1s, only 16 are associated with cases in the "large error" category (> 280.9 n mi). For GFS, six of the seven cases with statistically-significant PC1 values are cases with large 120-h errors. These GFS cases became the focus in the case studies that follow.

## C. CORRELATION OF PCS AND EOFS TO ERROR MAGNITUDE AND OBSERVED MODEL ERROR MECHANISMS: TWO CASE STUDIES

As a result of the fairly consistent correspondence between significant PC1 values for GFS in 500 hPa heights and TC forecast track errors, both of the following case studies considered GFS. Case A is an analysis of the high correlation of PC1 to EOF1 in both 500 hPa heights and vorticity during Typhoon Nesat in June 2005 (Figure 15a). The second case (Case B) is associated with a high negative correlation of PC1 to EOF1 in 500 hPa heights and vorticity during Typhoon Kirogi in October 2005 (Figure 15b). Both storms were located south of Japan. Case A is an example of excessive direct cyclone interaction and Case B is an example of excessive response to vertical wind shear (E-RVS).

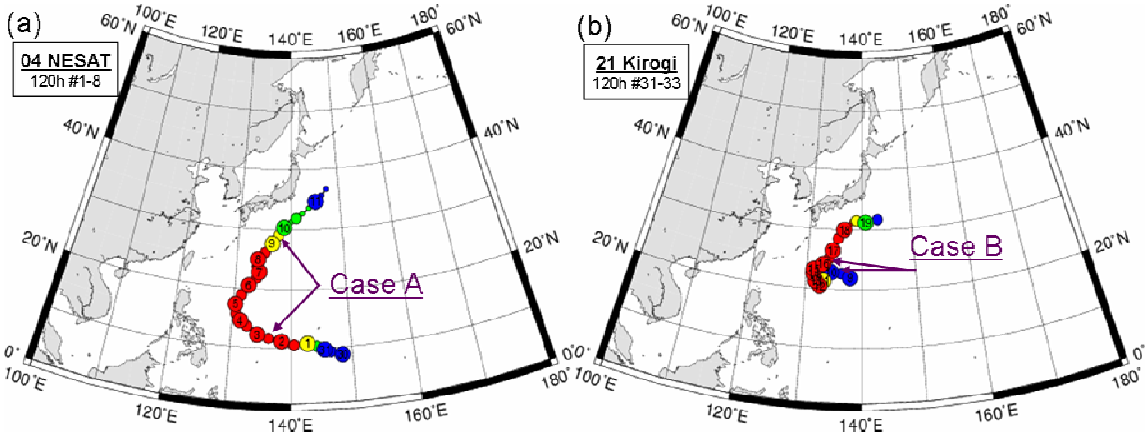

Figure 15. Best track data for case studies of (a) Typhoon Nesat (04W) and (b) Typhoon Kirogi (21W) (after http://agora.ex.nii.ac.jp/digital-typhoon/).

### 1. Case Study A: 120-h Cases 4-6 / Typhoon Nesat / E-DCI

The PC1 chart for 120-h 500 hPa heights (Figure 10) has significant positive coefficients to the EOF1 pattern for GFS (Figure 9) for cases 4, 5, and 6. The pattern in EOF1 has the TC in an area of higher heights, with an area of lower heights to the north. The resulting steering is eastward, which means that the GFS track is expected to deviate from the three-model mean track by that eastward component. Following the procedure in Chapter II, examining the individual model error magnitudes and directions reveals that GFS had the largest error (Figure 16a), and that the GFS forecast position was displaced to the northeast of the best track position (Figure 16b) in each of these cases. Since the EOF1 for 500hPa heights seems to be related primarily to the zonal component of the motion, it is assumed that the northward component of the motion is accounted for by another EOF.

Although Typhoon Nesat and an adjacent cyclone do not fully merge as described in the earlier DCI scenario (Figure 3), the GFS sea-level pressure forecast for case 4 incorrectly predicts the interaction of Typhoon Nesat with a midlatitude cyclone (Figure 17a-c). At the initial time of the forecast of case 4, Nesat was east of the Philippines and moving WNW. In the 72-h forecast (Figure 17b), Nesat was predicted to merge briefly with the midlatitude cyclone east of Taiwan, then accelerate to the northeast (NE) by 96 h (Figure 17c) and be SE of mainland Japan by 120 h. The verifying analyses (Figure 17d,e), have no indication of an interaction with a midlatitude cyclone in the East China

Sea. As a result, the movement of Nesat was actually much slower than that forecast by the GFS, and after 120 h, Nesat was south of Kyushu, which is well to the southwest (SW) of the GFS forecast position.

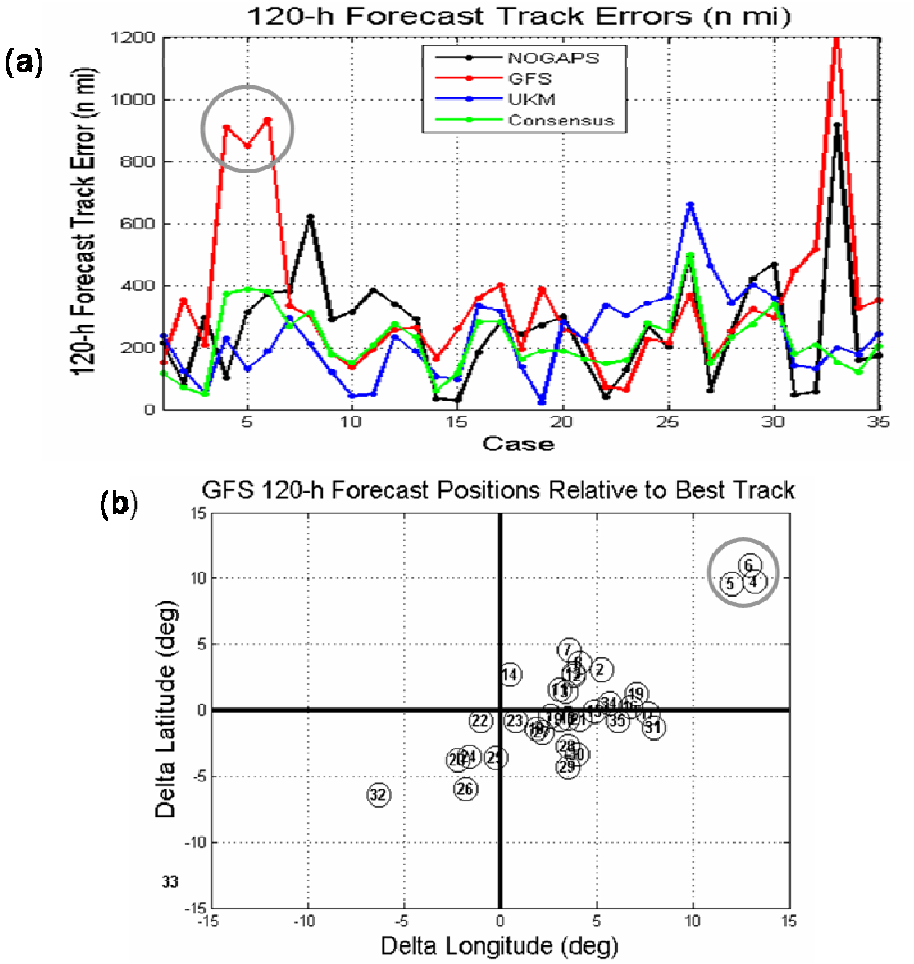


Figure 16. (a) Magnitude (n mi) of the 120-h forecast track errors for each model and the three-model consensus (see inset). (b) Direction error (n mi) relative to the best-track location, which is defined to be at the intersection of the two black lines. The gray circles highlight the magnitude of the error for cases 4-6 and the position relative to the center indicates the relative direction of the error for cases 4-6.

The positive statistically-significant PCs for 500 hPa heights correlate well with this E-DCI event. However, the correlation is not limited to this single variable. Although the signal from the 500 hPa vorticity EOF1 is not as strong as it was for heights, the PC1 values are statistically significant for cases 4-6 (Figure 8). The

associated EOF pattern for vorticity (Figure 7) is consistent with a SE deflection relative to the consensus TC motion. Since the forecast cyclone tracked NE, this EOF does not explain all aspects of the GFS error. However, the eastward component of the track deflection does remain consistent.

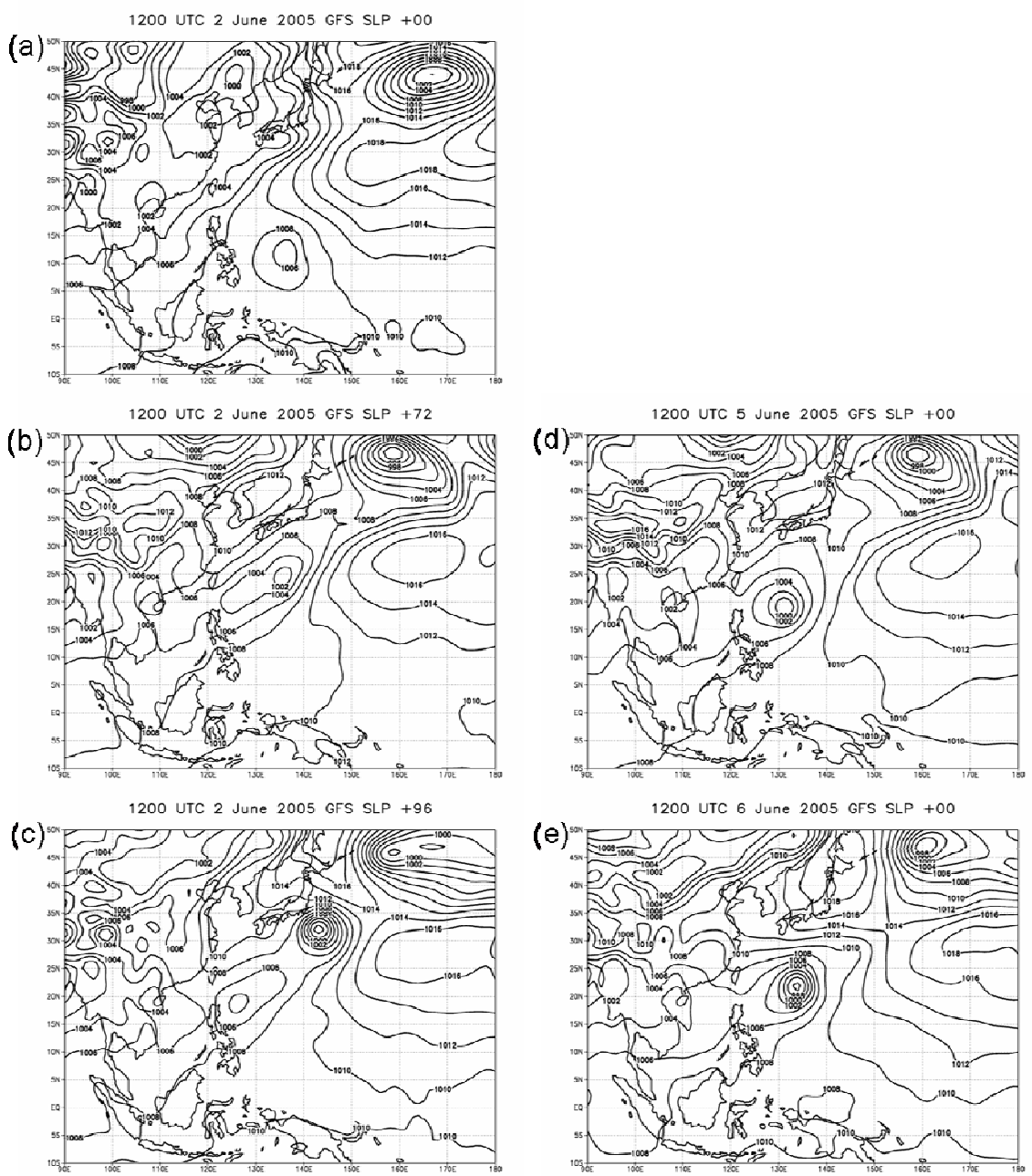


Figure 17. Sea level pressure fields for GFS at (a) 1200 UTC 2 June 2005 analysis, (b) 72-h forecast valid at 1200 UTC 5 June 2005, and (c) 96-h forecast valid at 1200 UTC 6 June 2005. (d),(e) verifying analyses for the corresponding times in (b),(c).

The association of the track deflections and the EOF patterns is clear in several succeeding EOFs and PCs as well. For example, the PC2 for 500 hPa heights (Figure 10) has a high negative correlation in case 6 to EOF2 (Figure 9). For a positive PC2, the EOF2 pattern has higher heights to the north, so when the signs are reversed, the resulting geostrophic motion is eastward, which again agrees with one component of the TC track error. However, not all higher order PCs and EOFs are in consistent agreement with the track error direction.

The correlation is also clear in the 500 hPa height PC1 at 72 h (Table 4), which is important because early diagnosis of high environment-to-error correlations may provide early warning of future large errors. After 72 h, two of the three pertinent cases have statistically-significant PC1 values for 500 hPa heights. In each case, the PC1 magnitude increases through the 96-h and 120-h forecasts and the error increases as well. The earlier and later cases (numbered 3 and 7 at 120 h) do not have statistically-significant PCs during any of the forecast times, and their errors are significantly lower.

Table 4. Trends for PC1 amplitude and track error growth in time for GFS 500 hPa height for 72-h, 96-h, and 120-h forecasts.

| Forecast Date-Time (YMD-UTC) | 72-h Case No. | 96-h & 120-h Case No. | 72-h 500 hPa HGT PC1 | 72-h GFS Error (n mi) | 96-h 500 hPa HGT PC1 | 96-h GFS Error (n mi) | 120-h 500 hPa HGT PC1 | 120-h GFS Error (n mi) |
|---|---|---|---|---|---|---|---|---|
| 2005060100 | 11 | 3 | 0 | 105.2 | 0.2 | 154.7 | 0.2 | 207.8 |
| 2005060212 | 13 | 4 | 1.7 | 396.6 | 1.9 | 760.9 | 2.1 | 910.1 |
| 2005060300 | 14 | 5 | 0.7 | 350.5 | 1 | 680.7 | 1.3 | 849.8 |
| 2005060312 | 15 | 6 | 1.2 | 605.4 | 2.2 | 682.3 | 3.1 | 936.5 |
| 2005060400 | 16 | 7 | 0.7 | 339.8 | 0.7 | 389.5 | 0.9 | 333.7 |

This analysis reveals the critical nature of the positive statistically-significant PCs for GFS. For the three variables examined (PCs 1 and 2 for 500 hPa heights and PC1 for 500 hPa vorticity), *every time* GFS had a positive statistically-significant principal component (cases 4, 5, and 6), the GFS TC track forecast had a large error. Examining the earlier and latter cases relative to these three cases, the principal components were not statistically significant, and the errors in the GFS forecast were much smaller (207.8 n mi

in case 3 and 333.7 n mi in case 7; Table 4). In this case, the statistically-significant positive correlations were coincident with the E-DCI cases that resulted in large 120-h errors.

A purpose of this study was to help the forecaster understand when incorrect modeling of the large-scale environment could be called "excessive" enough to remove the errant model from consideration and form a selective consensus forecast. Had the forecaster known that a statistically-significant positive PC value signified a large error when making his forecast, and chosen to not include the GFS model in an S-CON forecast, the consensus error would have decreased by more than 230 n mi in cases 4, 5, and 6 (Table 5). If additional case studies validate a positive correlation between this environmental pattern and the type of error mechanism and scope of error it indicates, this technique might allow the forecaster to distinguish those cases that will result in large-track errors.

Table 5. Hypothetical error reduction resulting from objective error mechanism identification in Case Study A.

| 120-h Case | N-CON Error (n mi) | (NGP, UKM) S-CON Error (n mi) | S-CON Error Reduction (n mi) | S-CON TC Track Forecast Improvement (%) |
|---|---|---|---|---|
| 4 | 373.5 | 94.9 | 278.6 | 74.6 |
| 5 | 389.1 | 153.3 | 235.8 | 60.6 |
| 6 | 379.7 | 90.0 | 289.7 | 76.3 |

### 2. Case Study B: 120-h Cases 32-33 / Typhoon Kirogi / E-RVS

The second case study focuses on the large significantly negative PC1 values for cases 32-33 for the GFS 500 hPa heights (Figure 9) and vorticity (Figure 7). As in Case A, this statistically-significant correlation corresponds to a significant error in the GFS forecast track (Figure 18a). In cases 32-33, these GFS forecast errors are well to the west and south of the verifying position (Figure 18b).

The negative sign of the principal component reverses the signs on the EOF pattern, which for 500 hPa heights places the TC in a trough with higher heights to the

north, and thus results in a westward steering component for the TC track. Note how the negative PC1 results in an exact inverse in track error direction (Figure 18b) compared to the previous case.

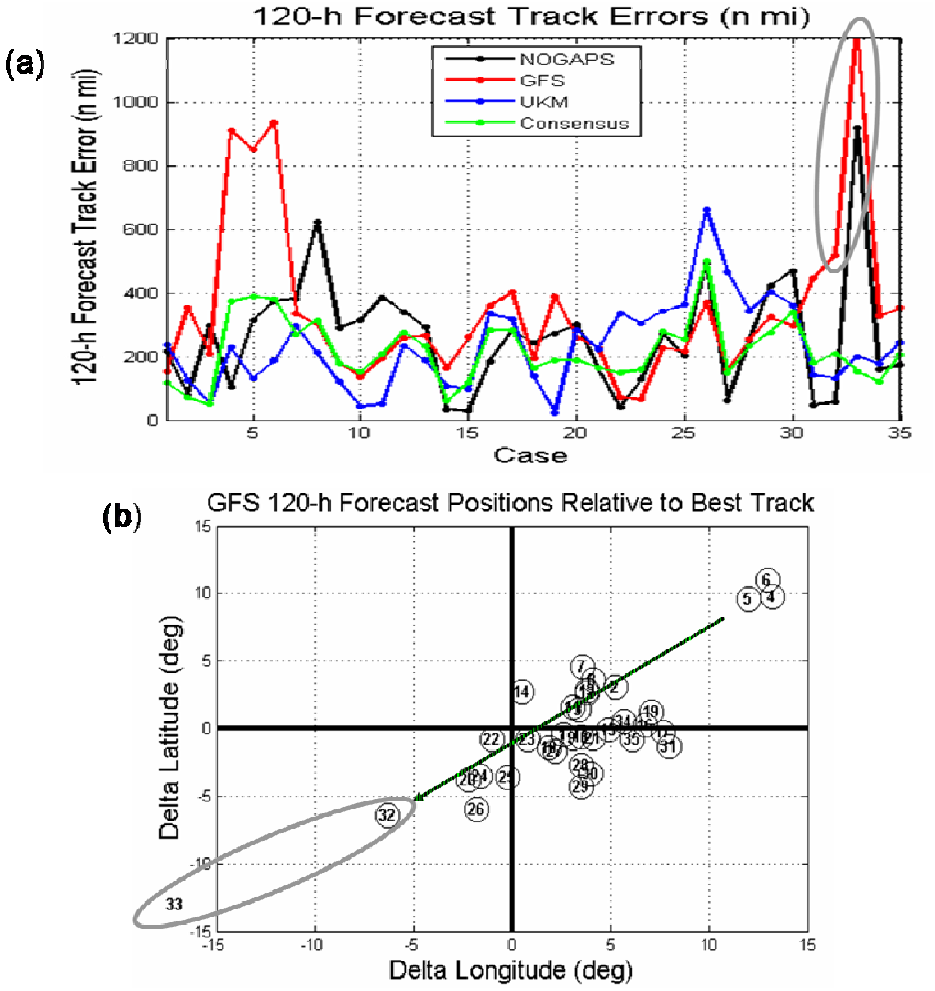


Figure 18. (a) Magnitude (n mi) of the 120-h forecast track errors for each model and the three-model consensus (see inset). (b) Direction error (n mi) relative to the best-track location, which is defined to be at the intersection of the two black lines. The gray circles highlight the magnitude of the error for cases 32-33 and the position relative to the center indicates the relative direction of the error for cases 32-33.

In this case, the error is caused by excessive response to vertical wind shear (E-RVS), which occurs because the GFS does not accurately predict the vertical structure of the typhoon (Payne 2006). Consequently, the modeled TC is not steered properly by the

500 hPa flow – or even the 700 hPa flow. The GFS sea-level pressure analysis (and subsequent forecast) for case 33 has the typhoon NE of the Philippines (not shown). The GFS model moves the storm toward NNW through 36 h and then fills it, while the tropical cyclone actually tracks NNE through the period.

The 700 hPa forecast heights illustrate clearly the E-RVS and the predicted excessive dissipation (Figure 19a-c). The midlatitude trough approaches from the northwest, deepens, and deflects the TC to the NE (Figure 19d). In the GFS forecast, the upper portion of the TC is advected downstream, which leaves the low center exposed and it then is dissipated due to the interaction. In the forecast, the TC is no longer vertically coherent at 72 h (Figure 19b), and the low-level center is predicted to move to the SW, while the TC actually continues to move NE under the influence of the midlatitude trough. The GFS 700hPa height 120-h forecast has no remaining evidence of the TC (Figure 19c), while the typhoon is actually SE of Kyushu (Figure 19e).

Cases 32 and 33 also have significantly negative PC1 values for the 500 hPa vorticity (Figure 8). As in the case study A, the EOF1 pattern can explain one component of the track error (Figure 18b), but not the other component. The negative PC1 for the vorticity EOF1 (Figure 7) results in a northwest component to the TC motion. Here the westward component of the error can be explained, but the northward component is not explained by EOF1.

Cases 32 and 33 also have significantly negative PC1s for the 700 hPa heights. The resulting motion inferred from the associated EOF (Figure 11) is toward the NW, so again only one component of the SW error is explained. Additionally, for EOF modes 2 and 3 only two of the eight PCs have statistically-significant amplitudes for cases 32-33. Case 33 has a slightly positive PC2 for 700 hPa heights, and a significantly negative PC2 for 700 hPa vorticity. The positive PC2 for the 700 hPa heights indicates a NW TC deflection, so again only one component of the error direction is correctly indicated. However, the track deflection inferred from the 700 hPa vorticity EOF does not correlate well to the direction of the error as it implies a NE component to TC motion. Since only one of the second and third PCs and EOFs provides the correct indication of the track error, these PCs and EOFs do not clarify the environment-to-error correlation. While the

EOF analysis for cases 32-33 did explain some aspects of the large 120-h errors by the GFS model, the statistically-significant principal components did not explain as much of the error in this case study as it did in Case A.

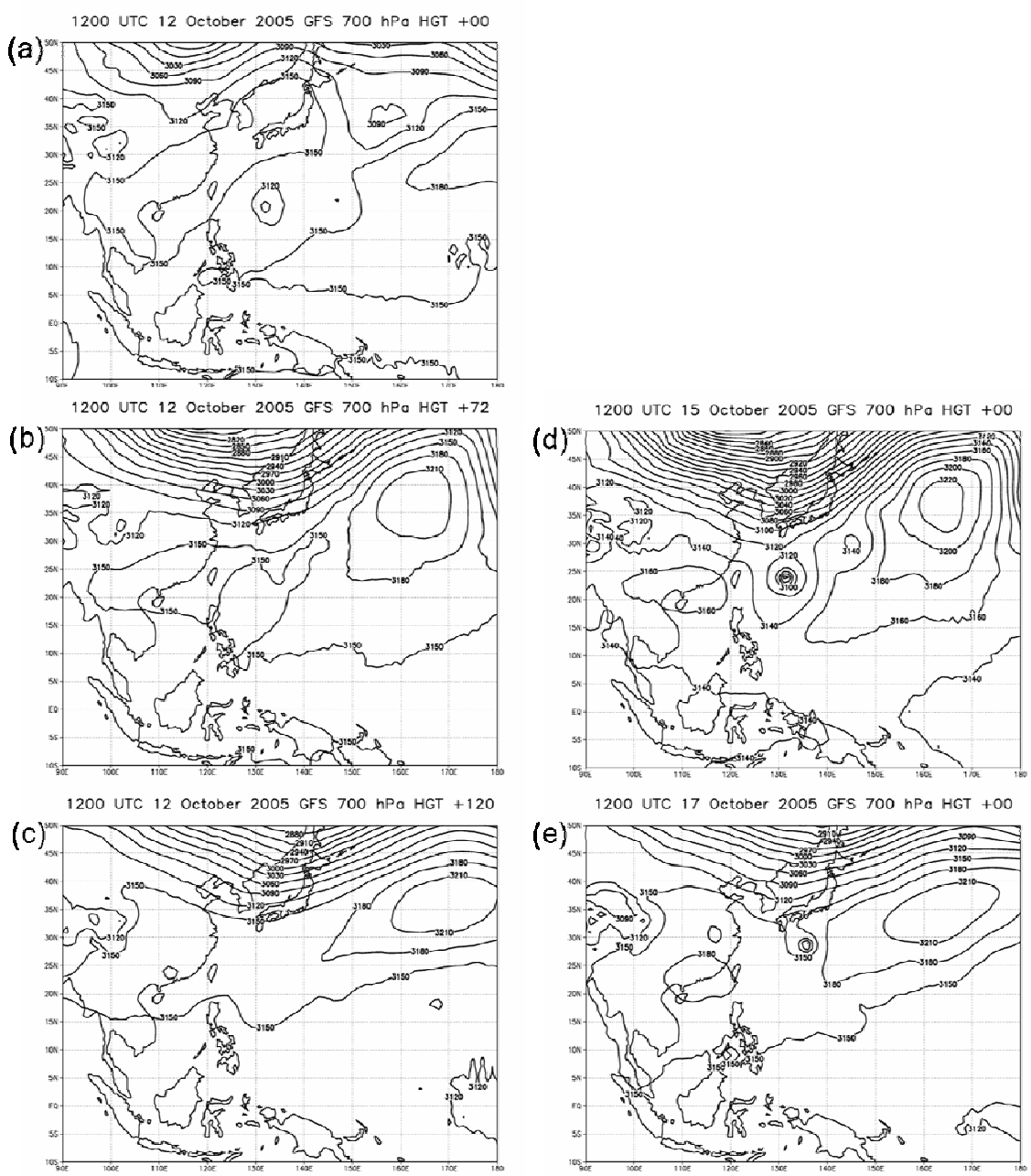


Figure 19. Height fields at 700 mb from the GFS (a) 1200 UTC 12 October 2005 analysis, and (b) 72-h forecast valid at 1200 UTC 15 October 2005, and (c) 120-h forecast valid at 1200 UTC 17 October 2005. (d),(e) verifying analyses for the corresponding times in (b),(c).

Case 18 also had statistically-significant negative PC1 amplitude for 500 hPa heights (Figure 18), yet it was not an instance of E-RVS. It is noteworthy that case 18 was a SSSE case, and it is expected that the forecaster would have followed the non-selective consensus in a small-spread case.

Should the forecaster have chosen to make a selective consensus forecast in cases 32-33 by rejecting the GFS track forecast, no net reduction in TC track forecast error would have been realized, and in fact the 120-h track error would have been increased by about 35 n mi. Although case 32 was categorized in a LSME tercile and case 33 was characterized in a LSLE tercile using the mean model errors, the N-CON error for both of these cases was small. Since the GFS and NOGAPS forecasts had errors in opposite directions, these errors compensated, which indicates the need to pursue objective analysis of the environmental patterns and error magnitude and mechanisms in other models as well.

THIS PAGE INTENTIONALLY LEFT BLANK

# IV. SUMMARY AND FUTURE DIRECTIONS

The objective of this study was to determine if information derived from storm-relative EOFs of dynamical model fields associated with large-error track forecasts would be sufficiently different from the principal components associated with lower-error and lower-spread cases such that an objective determination could be made that a selective consensus should be formed. Objective analysis yielded principal component signs and magnitudes that were consistent with the spread of individual model forecast tracks. In two case studies, the PCs identified the environmental patterns that were consistent with the TC track forecast error. That is, statistically-significant principal components for the GFS corresponded well to cases with large TC track forecast errors. With this information, the JTWC forecaster could hypothetically improve his track forecast accuracy by more than 230 n mi in Case Study A.

The amplitude of PCs indicates spread among model fields. A statistically-significant PC amplitude implies a significant differential pattern that results from the model field being quite different from the three-model mean (which would also result in a different environmental steering mechanism for the TC). In this study, medium- and large-spread cases were more apt to have multiple statistically-significant PCs, since in those cases multiple models deviated from the mean pattern and their strong anomaly patterns were represented well by the EOFs. In small-spread cases, the variability was less apparent in the EOF1 mode and became more evident in the second and third EOFs, as the PCs increased in statistical significance.

While a noteworthy correspondence occurred between the sign change in PC1 for GFS and the 180 shift in error direction between cases 4 and 33, an improved direction-correlation technique is required to correlate error direction to the best-track position to improve the reliability and accuracy of the error direction prediction. The potential to effectively influence the forecaster's decision to make a selective consensus in large-spread cases remains intact, as it has been shown that the magnitude of the PCs can be correlated to the magnitude of the spread among TC track forecasts. Furthermore,

outlying PC values have been identified with the errant model track, which is an important factor in determining whether an S-CON should be formed.

Upon completion of appropriate research, the operational deliverable of this objective analysis environmental-pattern-to-TC-track-error correlation technique is to provide a quality indicator to the forecaster for each model at each forecast time. The goal is for the forecaster to have a reliable indicator that characterizes how well that model has performed in that environment over time. To achieve this, each variable at each level must be assigned a certain weight with regard to its impact on TC steering. These weights would then be applied based on the objective analysis – a value determined by the correlation between the PC amplitude and the resulting error magnitude – for each variable. Although this study has demonstrated feasibility, quantifying the correlation for each parameter at each time step has yet to be completed.

Several studies are recommended to follow this first attempt at correlating environmental patterns to tropical cyclone forecast track errors. Future work will need to address the following questions: Will the detectability and predictability of error mechanisms hold when the relative positions of the member models differ? Will the same relationships between PC magnitudes and signs and the TC tracks hold with the increased stability resulting from a significant increase in the number of cases? Are other environmental patterns related to error magnitudes and mechanisms detectable? How well will this technique work when the numerical models are modified? Can this approach be used to more accurately forecast certain stages of a TC lifecycle (formation, recurvature, etc.)? However, the primary question is: can the EOF PCs be used with a Linear Discriminant Analysis to provide high probabilities that the track is likely to be erroneous and be discarded to form a selective consensus?

The military and civilian impacts of tropical cyclones necessitate mitigation to the greatest extent possible. Recent first-hand experience along the Gulf of Mexico has forever etched these impacts into the memory of this generation. The challenge facing the meteorology community is to provide accurate TC track forecasts as far in advance as possible to convey the threat of an impending natural disaster and thereby motivate the affected population to take appropriate action. This study has illustrated that objective

analysis offers an opportunity to improve the accuracy of 120-h TC track forecasts, which is a critical step toward mitigating risk and minimizing damage caused by tropical cyclones.

THIS PAGE INTENTIONALLY LEFT BLANK

# LIST OF REFERENCES


Carr, L.E., and R.L. Elsberry, 2000a: Dynamical tropical cyclone track forecast errors. Part I: Tropical region error sources. *Wea. Forecasting*, **15**, 641-661.

Carr, L.E., and R.L. Elsberry, 2000b: Dynamical tropical cyclone track forecast errors. Part II: Midlatitude circulation influences. *Wea. Forecasting*, **15**, 662-681.

Elsberry, R.L., and L.E. Carr, 2000: Consensus of dynamical tropical cyclone track forecasts – error versus spread. *Mon. Wea. Rev.*, **128**, 4131-4138.

Goerss, J.S., 2000: Tropical cyclone track forecasts using an ensemble of dynamic models. *Mon. Wea. Rev.*, **128**, 1187-1193.

Goerss, J.S., C.R. Sampson, and J.M. Gross, 2004: A history of western North Pacific regional tropical cyclone track forecast skill. *Wea. Forecasting*, **19**, 633-638.

Jeffries, R. A., and E.J. Fukada, 2002: Consensus approach to track forecasting. Paper TP 3.2, Extended Abstracts, *Fifth International Workshop on Tropical Cyclones*, Cairns, Australia, World Meteorological Organization (Geneva).

Kehoe, R.M., 2005: Characteristic errors in 120-h tropical cyclone track forecasts in the western North Pacific. M.S. Thesis, Naval Postgraduate School, 115 pp. [available at http://library.nps.navy.mil/uhtbin/hyperion/05Mar%5FKehoe.pdf, accessed 20 September 2006.]

Payne, K.A., 2006: Evaluation of causes of large 96-h and 120-h track errors in the western North Pacific. M.S. Thesis, Naval Postgraduate School, 89 pp. [available at http://library.nps.navy.mil/uhtbin/hyperion/06Jun%5FPayne.pdf., accessed 20 September 2006.]

Richman, M.B., 1986: Rotation of principal components. *J. Climatol.*, **6**, 293-335.

Sampson, C.R., J.A. Knaff, and E. M. Fukada, 2006: Operational evaluation of a selective consensus in the western North Pacific basin. *Wea. Forecasting*, in review.

THIS PAGE INTENTIONALLY LEFT BLANK

# INITIAL DISTRIBUTION LIST

1. Defense Technical Information Center
   Ft. Belvoir, Virginia

2. Dudley Knox Library
   Naval Postgraduate School
   Monterey, California

3. Professor Russell L Elsberry
   Naval Postgraduate School
   Monterey, California

4. Associate Professor Patrick A. Harr
   Naval Postgraduate School
   Monterey, California

5. Elizabeth R. Sanabia
   Naval Postgraduate School
   Monterey, California

6. Director, Joint Typhoon Warning Center
   Naval Pacific Meteorology and Oceanography Center
   Pearl Harbor, Hawaii